Perea García, A.; Garcia Molina, A.; Andres-Colas, N.; Francisco José Vera Sirera; Perez Amador, MA.; Puig, S.; Penarrubia, L. (2013). Arabidopsis copper transport protein COPT2 participates in the crosstalk between iron deficiency responses and low phosphate signaling. Plant Physiology. 162(1):180-194. doi:10.1104/pp.112.212407.

Running Head:

COPT2 responds to iron and phosphate deficiencies

Corresponding Author:

Lola Peñarrubia.

Departament de Bioquímica i Biologia Molecular. Universitat de València. Av. Doctor Moliner, 50. E-46100 Burjassot, Valencia, Spain.

Tel: +34-963543013

Fax: +34-963544635

E-mail: penarrub@uv.es

Research Area:

Environmental Stress and Adaptation

Associate Editor:

Julia Bailey-Serres

Title:

***Arabidopsis* copper transport protein COPT2 participates in the crosstalk between iron deficiency responses and low phosphate signaling**

Authors:

Ana Perea-García[1**], Antoni Garcia-Molina[1# **], Nuria Andrés-Colás[1], Francisco Vera-Sirera[2], Miguel A. Pérez-Amador[2], Sergi Puig[1‡], and Lola Peñarrubia[1]*.

Institution address:

[1]Departament de Bioquímica i Biologia Molecular. Universitat de València. Av. Doctor Moliner, 50. ES-46100 Burjassot, Valencia, Spain.

[2]Instituto de Biología Molecular y Celular de Plantas, Consejo Superior de Investigaciones Científicas-Universidad Politécnica de Valencia, ES-46022 Valencia, Spain

Footnotes:

This work was supported by grants BIO2011-24848 and CSD2007-00057 to L. P. from the Spanish Ministry of Economy and Competitiveness and by FEDER funds from the European Union. A. P.-G and A. G.-M. were recipients of a predoctoral FPI fellowship from the Spanish Ministry of Economy and Competitiveness

#Present address:
Molecular Plant Genetics Department. Max Planck Institute for Plant Breeding. Carl-von-Linne-Weg, 10. D-50829 Cologne, Germany.

‡ Present address:
Departamento de Biotecnología. Instituto de Agroquímica y Tecnología de Alimentos (IATA-CSIC). Av. Agustín Escardino 7, E-46980 Paterna (Valencia) Spain.

*Corresponding author e-mail: penarrub@uv.es
**These authors contributed equally to this work

One sentence summary: The function of the COPT2 high affinity copper transport protein unveil its role in the crosstalk among Cu, Fe and Pi deficiency responses in Arabidopsis.

ABSTRACT

Copper and iron are essential micronutrients for most living organisms because they participate as cofactors in biological processes, including respiration, photosynthesis and oxidative stress protection. In many eukaryotic organisms, including yeast and mammals, copper and iron homeostases are highly interconnected; yet such interdependence is not well-established in higher plants. Here we propose that COPT2, a high-affinity copper transport protein, functions under copper and iron deficiencies in *Arabidopsis thaliana.* COPT2 is a plasma membrane protein that functions in copper acquisition and distribution. Characterization of the *COPT2* expression pattern indicates a synergic response to copper and iron limitation in roots. We characterized a knockout of COPT2, *copt2-1*, which leads to increased resistance to simultaneous copper and iron deficiencies, measured as reduced leaf chlorosis and improved maintenance of the photosynthetic apparatus. We propose that COPT2 could play a dual role under Fe deficiency. First, COPT2 participates in the attenuation of copper deficiency responses driven by iron limitation, possibly to minimize further iron consumption. Second, the global expression analyses of *copt2-1* line versus wild-type Arabidopsis plants indicate that low phosphate responses increase in the mutant. These results open up new biotechnological approaches to fight iron deficiency in crops.

INTRODUCTION

Copper (Cu) and iron (Fe) act as a double-edged sword in living beings since they are essential redox active micronutrients, but are cytotoxic when in excess. Since both metals participate as catalytic cofactors in multiple metabolic pathways, their homeostasis needs to be strictly controlled. Plants are the basis of trophic chains and their nutritional deficiencies are often transferred to consumers. The essentiality of Cu and Fe in plants is evidenced by the symptoms that their deficiencies provoke, which affect the yield and nutritional value of crops (Märschner H., 2002; Puig et al., 2007). In biological terms, use of Fe preceded Cu due to the high bioavailability of Fe as Fe^{2+} under anoxic conditions. However, the appearance of oxygen in the atmosphere caused not only reduced Fe bioavailability, but also concomitantly increased the bioavailability and use of Cu by biological systems (Crichton and Pierre, 2001). In parallel with the incorporation of Cu into multiple processes requiring higher redox potentials, a fact that temporally coincided with the commencement of pluricellularity, new strategies to solubilize and acquire Fe^{3+} were developed. In some cases, enzymes that catalyze the same biochemical reaction are coordinately regulated to allow the alternative use of either Cu- or Fe-containing proteins, depending on metal bioavailability. One main example in *Arabidopsis thaliana* plants is the use of Cu and zinc (Zn) superoxide dismutase (Cu/ZnSOD) versus FeSOD, which both play a role in reactive oxygen species detoxification (Abdel-Ghany et al., 2005; Yamasaki et al., 2007; Burkhead et al., 2009; Waters et al., 2012).

In Arabidopsis, deciphering responses to Cu deficiency is now starting (Pilon et al., 2009; Penarrubia et al., 2010). A family of high-affinity Cu transport proteins, denoted COPTs in plants (CTR in yeast and humans), participates in Cu transport toward the cytosol. COPT1 is a plasma membrane-located member of this family that plays a key role in Cu uptake, root growth and pollen development (Kampfenkel et al., 1995; Sancenon et al., 2004). Recent studies have shown that deregulated Cu transport in *COPT1* overexpressing plants affects development under continuous environmental conditions (Andres-Colas et al., 2010). On the other hand, Cu activates calcium- and potassium-permeable plasma membrane transporters in *COPT1* overexpressing plants under 10 μM Cu conditions, a fact that might be caused by the generation of cytosolic hydroxyl radical (Rodrigo-Moreno et al., 2012). In the COPT family, *COPT1* and

COPT2 mRNA levels are down-regulated by Cu and their expression completely rescues the respiratory defect of *Saccharomyces cerevisiae ctr1Δctr3Δ* mutants, which are defective in high-affinity Cu uptake (Sancenon et al., 2003). Arabidopsis genome encodes a 17-member Zn finger plant-specific transcription factor family named SPL (SQUAMOSA-promoter binding-like proteins) (Birkenbihl et al., 2005). SPL7 has been shown to be essential for the transcriptional activation observed in response to Cu deficiency *in vivo* through its binding to the GTAC motifs within the promoter of Cu-responsive genes, including those encoding COPT1, COPT2 and Fe superoxide dismutase FSD1 (Yamasaki et al., 2009; Bernal et al., 2012).

Despite its abundance in soils, Fe bioavailability is very limited, which often provokes Fe deficiency symptoms (i.e., chlorosis) and lowers crop yields. The primary response of Arabidopsis plants to Fe deficiency is controlled through coordinated transcriptional activation, including the increased expression of metal reductases and transporters, such as *FRO2* and *IRT1* respectively, to improve metal bioavailability and acquisition. The Arabidopsis basic helix-loop-helix (bHLH) transcription factor bHLH29/FRU, also known as FIT (Fe deficiency-induced transcription factor), controls some of the root responses upon Fe limitation at different levels (reviewed by (Guerinot, 2000; Hindt and Guerinot, 2012; Ivanov et al., 2012)).

Fe availability has been shown to play a crucial role in the root architecture changes induced by phosphate (Pi) deficiency in Arabidopsis (Ward et al., 2008). Thus, whereas primary root elongation is greatly inhibited by Pi starvation, root growth is restored under reduced Fe without increasing Pi availability (Ward et al., 2008). Moreover, Pi-starved Arabidopsis plants show elevated Fe accumulation in both shoots and roots (Misson et al., 2005; Ward et al., 2008). Phosphorus is not only an essential macronutrient, but also a key component of, among others, membrane phospholipids, and is crucial for processes such as signaling cascades (Raghothama, 1999; Chiou and Lin, 2011). It has been suggested that Pi may be sensed indirectly via complex and antagonistic interactions between Pi and Fe availabilities, which still remain to be elucidated (Abel, 2011).

Given their sessile nature, plants are organisms that probably explore the widest variety of responses to environmental nutrient availabilities, and they have developed multiple regulatory mechanisms to respond to metal and nutrient deficiencies. In addition to the aforementioned substitution of specific metalloproteins, improved metal

bioavailability and acquisition, including the increased expression of metalloreductases and high-affinity transporters, are among the main strategies to help face metal deficiencies (Jeong and Guerinot, 2009; Palmer and Guerinot, 2009; Puig and Penarrubia, 2009). Nutrient status information has to be communicated between organs to optimize essential inorganic nutrient allocation, especially in plants growing under suboptimal conditions. Root architecture is differentially modified during nutrient deficiencies. Whereas root elongation is considered an adequate modification under metal deficiencies, possibly to seek metals in underground soil layers, the inhibition of primary root growth and the development of secondary and higher-order roots under Pi starvation maximize the interception of the nutrient in top soil layers (Liao et al., 2001). These processes exemplify not only the extensive crosstalk between different metals and other nutrient homeostasis networks, but also the delicate balance that plant cells have to strike according to the variable nutritional status in the environment.

In this study, we analyzed the function of high-affinity Cu transport protein COPT2, whose expression in Arabidopsis is up-regulated in roots by both Cu and Fe deficiencies (Sancenon et al., 2003; Colangelo and Guerinot, 2004; Waters et al., 2012), whereas Pi-starvation diminishes its expression (Thibaud et al., 2010). The phenotypes and gene expression changes displayed by a *copt2-1* line unveil a role for COPT2 in the crosstalk among Cu, Fe and Pi deficiency responses in Arabidopsis.

RESULTS

High-affinity copper transport protein COPT2 localizes to the plasma membrane of Arabidopsis cells.

The *COPT2* gene (*At3g46900*) from Arabidopsis encodes a protein with a 78% identity with COPT1 (Kampfenkel et al., 1995; Sancenon et al., 2003); see Figure S1A. The hydrophobicity pattern and the topological comparison between COPT2 and other CTR/COPT family members indicate the presence of three transmembrane domains (TMDs) with an external amino terminus and a cytosolic carboxy terminus (Figure S1B). Moreover, it possesses the conserved extracellular methionine residue (indicated by an asterisk in Figure S1) before TMD1, the MxxxM motif in TMD2 and the GxxxG motif in TMD3, which are essential in yeast homologs (Puig et al., 2002; Aller et al., 2004). A CxC motif is also observed in the COPT2 carboxy-terminal domain (Figure S1). Given its ability to fully complement the respiratory defects of yeast *ctr1Δctr3Δ* mutants and its regulation by environmental Cu in Arabidopsis, it has been previously suggested that both the COPT2 and COPT1 proteins could function in Cu acquisition in the plasma membrane of specific plant cells (Kampfenkel et al., 1995; Sancenon et al., 2003; Sancenon et al., 2004).

For the purpose of localizing COPT2 at the subcellular level in Arabidopsis cells, its coding sequence was fused to the green fluorescent protein (*COPT2-GFP*) under the control of the constitutive *CaMV35S* promoter. As shown in Figure 1A, the construct *COPT:GFP* complements the respiratory defect of yeast *ctr1Δctr3Δ* mutants to a similar extent as *COPT2* and *COPT1*, indicating that addition of the GFP does not interfere with the Cu transport function in yeast. Isolated Arabidopsis protoplasts transiently expressing the P*CaMV35S:COPT2:GFP* construct were analyzed for localization of COPT2-GFP, lipophilic styryl dye FM4-64 and chlorophyll fluorescences indicated by green, cyan and magenta colors, respectively (Figure 1B). In addition to the chlorophyll autofluorescence, *COPT2-GFP*-expressing cells display a signal on the cell surface that is absent in vacuoles, the cytosol and other discrete subcellular localizations. This signal colocalizes with the FM4-64 marker, which localizes to the cell surface at low temperatures (Figure 1B). Furthermore, immunofluorescence labeling of stable transgenic Arabidopsis plants expressing the

CaMV35S:COPT2-HA construct show a signal restricted to the peripheral side of the cytoplasm when using anti-HA antibodies (Figure S2). These results strongly suggest that the COPT2 protein localizes to the plasma membrane of Arabidopsis cells.

The *COPT2* expression is differentially regulated by Cu and Fe deficiencies.

In order to study the *COPT2* spatial expression pattern, the promoter region (P*COPT2*, covering 1248 base pairs upstream from the start codon) was fused to the *uidA* (*GUS*) reporter gene. The transgenic Arabidopsis lines harboring the P*COPT2:GUS* chimeric gene were obtained. GUS staining in 7-day-old Arabidopsis seedlings grown under Cu-deficient conditions indicated that *COPT2* was expressed in most tissues of the seedlings (Figure 2A). For roots, GUS staining was observed in the differentiation zone, but was absent from the elongation and meristematic zones (Figure 2B and 2C). Moreover, *COPT2* expression in roots included the lateral roots and root hairs, displaying expression mostly in the epidermis (Figure 2D). In cotyledons, the highest expression was observed in vascular bundles and hydathodes (Figure 2E). Histological analyses of seedlings and adult plants showed a *COPT2* promoter-driven GUS expression in the apical meristem and trichomes (Figure 2F) and in young leaves (Figure 2G). During the development of reproductive organs, the GUS staining in anthers (Figure 2H) indicates that *COPT2* is highly expressed in pollen (Figure 2I). Three other independent P*COPT2:GUS* lines were analyzed and showed the same *COPT2* tissue pattern expression (data not shown). A schematic *COPT2,* as compared to the *COPT1* expression pattern, along with other characteristics of both permeases, are shown in Figure S3.

The analysis of the regulatory elements in the P*COPT2* region indicates the presence of four GTAC motifs, which are probably involved in its regulation by Cu (Figure S4; (Yamasaki et al., 2009)). Interestingly, COPT2 is the COPT family member whose expression was most highly regulated by Cu deficiency (Sancenon et al., 2003; Yamasaki et al., 2009; del Pozo et al., 2010). In addition, a putative E-box consensus, which may be involved in the interaction with bHLH-type transcription factors such as the Fe-responsive FIT protein (Hartmann et al., 2005), was present in its promoter (Figure S4). Accordingly, *COPT2* expression has been shown to respond to Fe deficiency in a partially FIT-dependent manner (Colangelo and Guerinot, 2004). To ascertain *COPT2* expression under separate Fe and Cu deficiencies, or when both

deficiencies are applied simultaneously, wild-type (WT) seedlings were grown in the four following media combinations: first, Fe- and Cu-sufficient medium (+Fe+Cu; ½ MS supplemented with 10 μM $CuSO_4$); second, Fe-sufficient and Cu-deficient medium (+Fe-Cu; ½ MS without $CuSO_4$); third, Fe-deficient and Cu-sufficient medium (-Fe+Cu; ½ MS without Fe and supplemented with 10 μM $CuSO_4$ and 300 μM ferrozine, a specific Fe^{2+} chelator); and fourth, Fe- and Cu- deficient medium (-Fe-Cu; ½ MS without Cu and Fe, and supplemented with 300 μM ferrozine). The Cu concentration used in this experiment was 10 μM, which was high enough to guarantee a sufficient Cu supply while being far from the deficiency and excess responses (Andres-Colas et al., 2010). *COPT2* expression was induced by Cu deficiency (35.6-fold), by Fe deficiency (4.3-fold) and its expression was further increased under simultaneous Fe and Cu deprivation (52.3-fold) (Figure 3A and Table S1). *COPT2* expression remained mostly under the control of the SPL7 transcription factor since the *spl7* mutant displayed a significant drop at the mRNA levels (Figure 3A; (Yamasaki et al., 2009; Bernal et al., 2012)). However, *COPT2* was still expressed at low basal levels under all the conditions tested in the *spl7* mutant as compared to a *copt2* null mutant (*copt2-1* line, see next section) (Figure 3A), indicating that this basal expression level was SPL7-independent. Furthermore, the *COPT2* tissue pattern shows that under Cu deficiency (+Fe-Cu), it was highly expressed in roots and that its expression increased under both metal deficiencies (-Fe-Cu) (Figure 3B). In order to further define where *COPT2* expression started, root photographs under 1 h at 37ºC for GUS staining were obtained, showing cell patches of differentiated root cells (Figure 3B). Interestingly, high (1 μM) Cu levels (+Fe+Cu) completely abolished *COPT2* expression in roots, but a low expression level, which requires overnight GUS staining remained restricted to cotyledons under Fe deficiency (-Fe+Cu) (Figure 3B). The expression in roots requires Cu deficiency conditions, and it was not observed under Fe deficiency when the Cu levels in the medium were higher than 0.25 μM (Figure S5). However, the low expression in cotyledons was observed at higher Cu levels under overnight GUS staining conditions (Figures 3B and S5). Taken together, these results not only demonstrate that *COPT2* expression is differentially regulated by low Cu and Fe conditions, but suggest a crosstalk between both metal deficiencies.

Characterization of *copt2-1* line under Cu and Fe deficiency conditions.

A *copt2-1* line (Figure S6) that contains the T-DNA insert at the -55 base pairs (in relation to the translation start codon), separating the four putative Cu regulatory GTAC motifs from the *COPT2* coding sequence (Figure S6A), shows no *COPT2* expression in seedlings grown on different Cu availabilities (100 μM BCS, and 0, 1, 5, or 10 μM $CuSO_4$) (Figure S6C). Moreover under the four conditions previously stated for Cu and Fe availability, the *COPT2* expression levels in the *copt2-1* line were below those found in the *spl7* mutant (Figure 3A). Therefore, we used the *copt2-1* mutant to study the function of this transporter in Arabidopsis.

Since *COPT2* displays different expression patterns under +Fe-Cu, -Fe+Cu and -Fe-Cu conditions, we studied the potential *copt2-1* phenotypes under these conditions as compared to the +Fe+Cu control media. Apparently the mutant did not seem to differ from the WT controls when grown on soil or in ½MS with different Cu availabilities. Furthermore certain parameters, such as root length, seed germination, de-etiolation and hypocotyls length, showed no significant difference between the WT and *copt2-1* line under the different Cu statuses analyzed (data not shown). However, whereas the WT plants grown under simultaneous Cu- and Fe-deficiency conditions exhibited a light green leaf appearance, a typical symptom of mild chlorosis, the *copt2-1* seedlings displayed a slight increased resistance to Fe deprivation by delaying symptoms, as shown by their greener leaves (Figure 4A). In order to quantify this *copt2-1* phenotype, total chlorophylls were measured in the 7-day-old WT and mutant seedlings grown under the four Fe/Cu conditions stated above. As Figure 4B illustrates, the *copt2-1* line showed increased chlorophylls when compared to the WT seedlings, especially under -Fe conditions. Despite no significant changes in fresh weight being detected under Fe deficiency (Figure S7A), a parameter indicative of photosynthetic apparatus integrity such as *LHCB1.1* (light harvesting complex B1.1) mRNA, showed a slightly higher level in the mutant than in the WT plants under Fe deficiency conditions (Figure S7B). In order to ascertain whether these defects were COPT2-specific, we transformed the *copt2-1* line with the *COPT2* WT gene driven by its own promoter (P*COPT2:COPT2:GFP*). Importantly, the P*COPT2:COPT2:GFP* seedlings grown under both metal deficiencies revealed a partial restoration of *COPT2* expression and, accordingly, displayed an increased sensitivity to metal deficiencies as shown by the chlorophyll content (Figure 5). Moreover, the *LHCB1.1* and *FSD1* expression decreased when compared to the *copt2-1* line under simultaneous metal deficiency (Figure 5C),

which is in agreement with reduced plant performance in the presence of *COPT2* expression. The *copt1* mutant also display a similar phenotype of resistance to Fe deficiency-induced chlorosis (results not shown), which further corroborates the role of Cu in this process. To investigate whether the better resistance of the mutant to ferric chlorosis under -Fe-Cu conditions was also displayed in adult stages, plants were grown in hydroponic cultures under +Fe+Cu (Hoagland) and -Fe-Cu conditions (Hoagland with no added Cu and Fe). As indicated for the seedlings grown in agar plates (Figures 4 and 5), once again the chlorosis under -Fe-Cu conditions in the aerial part was less pronounced or retarded in the *copt2-1* line than in the WT adult plants (Figures 6A and 6B). It is worth noting that the plastocyanin content in the leaves of the adult plants grown under -Fe-Cu conditions was higher in the *copt2-1* line than in WT plants (Figure S8). Moreover, senescence of the *copt2-1* siliques is delayed compared to WT (Figure S9A) and subsequently the mutant produces more seeds (Figure S9B) with a higher germination rate (40%) than WT plants (5%) when grown under both metal deficiency conditions. Taken together, these results further support the better or extended maintenance of the photosynthetic apparatus in the *copt2-1* line than in the WT plants grown under conditions of simultaneous Fe and Cu deficiencies, which leads to improved plant growth and seed production.

In order to determine whether the total endogenous metal content in these plants was responsible for the phenotypes observed in the *copt2-1* line, the Fe and Cu contents from the 7-day-old seedlings grown under the four Fe/Cu conditions described above were determined by inductively coupled plasma mass spectroscopy (ICP-MS). No significant differences in Fe content were observed between WT and *copt2-1* plants (Figure 7A). Although a slight decrease in Cu content was detected in the mutant under high Cu (Figure 7B), *COPT2* was expressed at low levels under these conditions (Figure 3A), questioning a putative COPT2 role in Cu uptake from the medium under high Cu. Moreover, no significant differences in Cu content between the WT and the *copt2-1* plants grown under either hydroponic or Cu deficiency conditions were found in different organs, such as roots, rosette leaves, stems or inflorescences (data not shown). These results suggest that the total endogenous metal content in seedlings is not responsible for the phenotype of the simultaneous resistance to Fe and Cu deficiencies displayed by the *copt2-1* line.

The negative effects of Fe starvation on Cu deficiency responses are altered in the *copt2-1* line.

In order to understand the molecular reasons underlying the *copt2-1* phenotype, the mRNA levels of selected genes regulated by Cu deficiency (*COPT1, FSD1* and *CSD2*) were determined by qPCR in the 7-day-old WT and mutant seedlings grown under the four Fe/Cu conditions described above (Figure 8). We observed that *COPT1* expression was up-regulated by Cu deficiency in both the WT and *copt2-1* lines (Figure 8A, +Fe+Cu *vs.* +Fe-Cu; (Sancenon et al., 2003). It is interesting to note that when Fe was limited (-Fe conditions), no *COPT1* up-regulation was observed in response to Cu deficiency (Figure 8A, -Fe+Cu *vs.* -Fe-Cu). These results suggest that Fe deficiency negatively affects *COPT1* induction by low Cu in both the WT and *copt2-1* lines. To further address this observation, we determined the mRNA levels of Cu-regulated genes *FSD1* and *CSD2,* which respectively encode for FeSOD and Cu/ZnSOD. As Figures 8B and 8C depict, the *CSD2*/*FSD1* substitution was normally observed with Cu deficiency under Fe-sufficient conditions (+Fe+Cu *vs.* +Fe-Cu). However, when Fe deficiency was imposed, the increased *FSD1* mRNA levels were greatly compromised (Figure 8B, -Fe+Cu *vs.* -Fe-Cu) and the *copt2-1* line showed a slightly increased *FSD1* expression under Cu and Fe deficiencies (Figure 8B). To check whether this slight increase in SOD expression implies a general enhancement in oxidative stress protection in the *copt2-1* line, SOD activities were measured in gel and no significant differences were found between the WT and the mutants (Figure S10A). Moreover, when subjected to oxidative treatments, such as hydrogen peroxide (500 μM) or paraquat (0.1 μM), no phenotypical differences were observed (Figure S10B), indicating that the *copt2-1* line does not show more resistance to general oxidative stress conditions.

Since Fe starvation attenuated the Cu deficiency-induced up-regulation of *COPT1* and *FSD1* (Figures 8A and 8B), we wondered how Cu deficiency could affect plant responses to Fe scarcity. For this purpose, the expression pattern of two well-known Fe deficiency genes, metalloreductase *FRO2* and Fe transporter *IRT1*, was analyzed under the four previously assayed Fe/Cu conditions. Although both genes were activated in response to Fe deficiency (Figures S11A and S11B, +Fe *vs.* -Fe), as previously reported (Colangelo and Guerinot, 2004), no major differences were observed in the expression of *FRO2* and *IRT1* in *copt2-1* plants (Figure S11).

Global analysis of gene expression changes under Fe and Cu deficiencies indicate that *copt2-1* plants display phosphate starvation responses.

With the aim of characterizing at the molecular level the causes of enhanced resistance to Fe deficiency and induced chlorosis in the *copt2-1* mutant, a global profiling analysis of gene expression under Fe and Cu deficiency was performed. To that end, WT and *copt2-1* seedlings were grown for 7 days under Fe and Cu sufficient conditions (+Fe+Cu) and compared to seedlings grown on medium without Fe and Cu (-Fe-Cu). Moreover, medium without Fe (-Fe+Cu) has been used as a control for Cu-complemented expression changes in the *copt2-1* line. In order to validate these growth conditions, we have previously confirmed by qPCR analysis the expression pattern of two genes previously known to be upregulated by Cu deficiency, *COPT2* (Sancenon et al., 2003) (Figures 3A and S12A) and *ZIP2*, a ZRT, IRT-like protein 2 transporter (Wintz et al., 2003) (Figure S12B).

Global profiling analysis of *copt2-1* and WT lines was carried out from four biological replicates grown in the three different conditions (+Fe+Cu, -Fe-Cu and -Fe+Cu). A median $\log_2$ ratio of 1 (2-fold difference in expression) was used as a cutoff criterion to compare the mutant with the WT under each condition. We identified 324 differentially expressed genes (Tables S1 and S2) distributed in 49 induced (ratio>1) and 275 repressed (ratio<1) genes in the *copt2-1* line in the three growth conditions (Figure 9A). Repressed genes are more abundant than induced in all the conditions. The condition -Fe+Cu shows the largest number of genes which expression is affected. Gene ontology analysis indicated that repressed genes include those of the abiotic stress and detoxifying processes, maybe reflecting the consequences of the dismantling photosynthetic apparatus taking place in the WT plants (Table S3) which may be delayed in the mutant. Interestingly, a significant percentage (35%) of the induced genes is related to Pi starvation responses based on bibliography (Table 1). Over-representation of this category in all three nutritional conditions indicated a general effect of COPT2 function in Pi starvation (Table S4). The ribo-regulators *At4*, *IPS1* and several SPX domain proteins are among the best-known genes induced in Pi-starved plants and they have been shown to participate in Pi homeostasis and signaling (Franco-Zorrilla et al., 2007; Duan et al., 2008; Thibaud et al., 2010; Chiou and Lin, 2011). Therefore, *At4* and *SPX1* expression was analyzed in the *copt2-1* line, confirming the

microarray results (Figure 9B). Moreover, these data underscore the intricate interactions between Fe and Pi deficiencies, since whereas *At4* is down-regulated by Fe deficiency in WT, *SPX1* expression remains mostly unaffected (Figure 9B). To check how Cu is implicated in Pi-starvation, we have grown WT and *copt2-1* seedlings in Pi-deficient media and under different Cu and Fe regimes. As shown in Figures 10A and 10B, *copt2-1* displays slightly larger roots than WT plants in all growth conditions, indicating a general insensitivity to Pi deficiency. Moreover, the *COPT2* expression pattern remains unaffected under Pi starvation (Figure 10C). Taken together, our results are compatible with a model where *COPT2* is involved in the antagonistic responses of metals and Pi deficiencies (Figure 11).

DISCUSSION

The conserved family of CTR/COPT proteins mediates high-affinity Cu transport in eukaryotic organisms (reviewed by (Puig et al., 2002; Kim et al., 2008; Nevitt et al., 2012)). Distinct COPT-family members have been characterized in the plant Arabidopsis. Whereas COPT1 is a plasma membrane protein that functions in root Cu uptake and pollen development, COPT5 is intracellularly localized and mediates Cu mobilization under severe deficiency conditions (Sancenon et al., 2004; Garcia-Molina et al., 2011; Klaumann et al., 2011). Previous studies have shown that COPT2 is the most similar COPT-family protein to COPT1, that both genes fully complement the Cu transport defect of yeast *ctr1Δctr3Δ* mutants, and that they are up-regulated in response to Cu deficiency in a SPL7-dependent manner by probably SPL7-binding to GTAC motifs in the *COPT1* and *COPT2* promoter regions (Sancenon et al., 2003; Yamasaki et al., 2009; Bernal et al., 2012). Here we show that, similarly to COPT1, the COPT2 protein localizes to the plasma membrane of Arabidopsis cells. Furthermore, both genes display a similar aerial expression pattern under slight Cu-deficient conditions (½ MS medium), including the expression in cotyledons from young seedlings, trichomes, anthers and mature pollen (Sancenon et al., 2004). These observations suggest that COPT1 and COPT2 might exhibit a partially redundant function in Cu homeostasis in the aerial part. A notable difference between COPT1 and COPT2 relies on their root expression pattern. *COPT1* is exclusively expressed in primary and secondary root tips (Sancenon et al., 2004), where overexpression activates plasma membrane OH^-–sensitive calcium and potassium channels and subsequent root apex signaling (Rodrigo-Moreno et al., 2012). However, *COPT2* is expressed in subapical root regions (Figure 2), where the activation of these channels is prevented (Rodrigo-Moreno et al., 2012), suggesting local and specific functions and subsequent signaling events of these transporters in Arabidopsis roots. Moreover, another key difference is the regulation of both genes under Fe deficiency. In low Cu media, whereas *COPT1* is downregulated (Figure 8A), *COPT2* expression is increased by Fe deficiency (Figure 3A).

In this sense, it is noteworthy that previous genome-wide expression studies in Fe-deficient roots were mostly performed under low Cu levels (Colangelo and Guerinot, 2004; Buckhout et al., 2009; Yang et al., 2010; Stein and Waters, 2011). These studies have shown that *COPT2* expression is up-regulated in response to Fe deficiency, which

has been further corroborated herein (Figures 3 and S5). However, the Fe deficiency-induced *COPT2* expression in roots is abolished by high Cu in media, although still present in shoots (Figures 3B and S5), suggesting a role for Cu in FIT-mediated responses in Arabidopsis roots. Recently, (Waters et al., 2012) reported increased *COPT2* expression in roots, but a decrease in rosettes for Fe deficiency under low Cu conditions. The remaining *COPT2* expression in cotyledons under -Fe+Cu (Figures 3B and S5) may be attributed to another putative Fe-deficiency network that differs from FIT and is not affected by high Cu levels. It is believed that the increase in endogenous Cu levels when Fe is low (Figure 7B) may occur to favor the cofactor supply to Cu-enzymes (e.g., Cu/ZnSOD), which substitute their Fe counterparts (e.g., FeSOD) to optimize the utilization of low Fe available in more important or irreplaceable Fe-dependent functions (Waters et al., 2012).

Surprisingly, parameters indicative of the photosynthetic apparatus status, such as chlorophyll content are higher in *copt2-1* than in WT plants (Figures 4 and 5) indicating that the absence of *COPT2* expression results in better plant performance, which is more relevant under both metals deficiencies (Figure S9). A putative explanation for this interesting phenotype is based on the observation that *copt2-1* plants display higher *FSD1* mRNA levels than the WT ones for combined Fe and Cu deficiencies (Figure 8B). However, a concomitant disadvantageous effect of *COPT2* expression resulting from diminished oxidative protection is not observed in the *copt2-1* line (Figure S10). Instead, the analysis of global expression changes in the *copt2-1* mutant suggests a complex scenario where different cuproproteins and maybe specific COPT-mediated signaling processes could be at the basis of the observed phenotype. One of the altered categories in the *copt2-1* line is the response to low Pi, which is mostly independent of the metal status (Tables 1 and S2 and Figure 9B). Our results unveil a role of COPT2-mediated Cu transport in Pi starvation signaling, which is in agreement with the down-regulated *COPT2* expression observed under Pi starvation conditions (Thibaud et al., 2010). Potential connections between Pi starvation responses and the homeostasis of other ions have been described (Abel, 2011; Chiou and Lin, 2011). Root responses to Pi starvation have been suggested to be an outcome of the complex interactions between Pi and other nutrients, essentially Fe (Svistoonoff et al., 2007; Ward et al., 2008). With simultaneous Fe and Pi deficiencies, a recovery in primary root elongation has been reported (Ward et al., 2008). Our results add Cu homeostasis to those interactions in which Fe deficiency and Pi starvation have

antagonistic effects by up-regulating or down-regulating *COPT2* expression, respectively (Figures 3A and 11; (Thibaud et al., 2010)).

COPT2 could participate in Pi sensing by Cu delivery to cuproproteins, such as multicopper oxidases LPR1 and LPR2, which have been involved in root growth responses to low Pi (Svistoonoff et al., 2007). Our results are compatible with a role of COPT2-mediated Cu transport in supplying Cu to these enzymes. In this sense, a slight increase in root length is observed in the *copt2-1* line as compared to the WT under low Pi conditions (Figure 10), which is consistent with the phenotype observed in *lpr1* and *lpr2* mutants (Svistoonoff et al., 2007). In addition these data reveal a putative complex COPT2-mediated role in Pi-starvation systemic signaling, such as *At4* and *SPX1* expression (Figure 9B), which still remains to be elucidated.

A putative explanation to the better maintenance of chlorophylls observed in the mutant can be postulated as an indirect effect through Pi-starvation responses. Indeed under Pi-limiting conditions, plants substitute phosphoglycerolipids by activating the genes for galactolipid biosynthesis (Kobayashi et al., 2009). Monogalactosyldiacylglycerol (MGDG) is an abundant lipid in chloroplast membranes (Shimojima and Ohta, 2011). Mutants affected in MGDG synthase show reduced chlorophyll content (Jarvis et al., 2000). Changes in lipid composition have already been shown to be involved in Cu deficiency responses in *Chlamydomonas reinhardtii* (Castruita et al., 2011). The genes induced in *copt2-1* plants suggest that phospholipids substitution for galactolipids could take place in the mutant (Tables 1, S2 and S4). Alternatively, a putative COPT2-mediated signaling event could be involved in chlorophyll degradation and consequently, this process would be retarded in the *copt2-1* line. In agreement with this suggestion other degradation processes, such as seed protein mobilization are also inhibited in the mutant (Tables S1 and S3). In addition, both the influence of Cu on ethylene perception (Hirayama et al., 1999) and the recently postulated role of a multicopper oxidase in Fe homeostasis (Bernal et al., 2012) also indicate different Cu functions, which could affect plant responses under Fe and Pi starvation (Romera and Alcantara, 1994; Hirsch et al., 2006).

Although more studies will be needed to further ascertain the relevance of COPT2 in these processes, this study opens up novel possibilities to help develop strategies to improve the growth, yield and nutritional quality of crops under environmental metal deficiencies. Along these lines, recent studies in rice indicate

certain COPT-family members, which are up-regulated by both Cu and Fe deficiency (Yuan et al., 2011), as potential targets for biotechnological improvement.

MATERIALS AND METHODS

Plant growth conditions and treatments

Seeds of *Arabidopsis thaliana*, ecotype *Columbia-0* (Col-0), were surface-sterilized and stratified for 2 d at 4°C and were germinated in ½ MS medium plates either including 1% sucrose (Murashige, 1962) or supplemented with the indicated concentrations of metal ions. For severe Cu-deficient conditions, the ½ MS medium was supplemented with 100 µM BCS (*Bathocuproinedisulfonic acid disodium*). In order to know the effects of both Cu and Fe deficiencies in plants, the components of the ½ MS medium were prepared separately according to the conditions: macronutrients (10 mM NH_4NO_3, 9.4 mM KNO_3, 0.37 mM $MgSO_4 \cdot 7H_20$, 0.62 mM KH_2PO_4 and 1.13 mM $CaCl_2$), micronutrients (50 µM H_3BO_3, 36.6 µM $MnSO_4 \cdot H_20$, 15 µM $ZnSO_4 \cdot 7H_20$, 0.57 µM $NaMoO_4 \cdot 2H_2O$ and 0.05 µM $CoCl_2 \cdot 6H_20$), 50 µM Fe-EDTA, 0.25 mM KI, 1 µM $CuSO_4 \cdot 5H_20$, 0.05% MES, 1% sucrose and 0.8% phytoagar; pH 5.7-5.8. 7-day-old seedlings were grown in Fe- and Cu-sufficient medium (+Fe+Cu, Fe-sufficient and Cu-deficient medium (+Fe-Cu), Fe-deficient and Cu-sufficient medium (-Fe+Cu) and Fe- and Cu-deficient medium (-Fe-Cu). Cu-excess medium was supplemented with 10 µM $CuSO_4 \cdot 5H_20$. Fe-deficient medium was supplemented with 300 µM ferrozine. With the Pi-deficient medium, KH_2PO_4 was not included in the macronutrients solution. To study sensitivity to others stresses, seedlings were grown in paraquat and H_2O_2 solution (0.1 µM and 500 µM, respectively). Seedlings were grown for 7 days with a 12 h photoperiod (65 µmol m^{-2} of cool-white fluorescent light) at 23ºC/16ºC temperature cycle. Hydroponic cultures were performed in the same photoperiod conditions from 3-4 true leaves seedlings grown in commercial soil, which were transferred to black boxes containing standard Hoagland solution (0.1 X), pH 5.8, as described by (Hermans et al., 2005). After a 14-day adaptation, the -Fe-Cu treatment (corresponding to a Hoagland medium without Cu and Fe sources) commenced. Media were changed weekly for 4-5 weeks. The chlorophyll content of the Arabidopsis seedlings and leaves from adult plants was determined by the trichlorometric method (Parsons, 1962). Root length was measured using the *Image J 1.42q software* (http://rsb.info.nih.gov./ij).

Functional complementation assays in yeast

The yeast *ctr1Δctr3Δ* mutant strain was transformed with p426GPD, or with a vector containing *COPT1*, *COPT2* or *COPT2:GFP*, and was assayed for growth on glucose (YPD: 1% yeast extract, 2% bactopeptone, 2% glucose), glycerol (YPEG: 1% yeast extract, 2% bactopeptone, 2% ethanol, 3% glycerol), and glycerol + Cu (YPEG supplemented with 100 μM $CuSO_4$) media solidified with 1.5% agar (Puig et al., 2002).

Metal accumulation measurements

Fresh Arabidopsis material was dried at 65ºC for 2 days and digested with 65% (v/v) HNO_3 at 80-90ºC. Digested samples were then diluted with Millipore H_2O (*Purelab Ultra*), and Cu and Fe contents were determined by ICP-MS at the Servei Central d'Instrumentació Científica (Universitat Jaume I, Castelló Spain).

SODs activity assay

Plant material was homogenized in an equal volume of ice-cold grinding buffer (50 mM potassium phosphate, pH 7.4, 0.1% BSA, 0.1% ascorbate, 0.05% β-mercaptoethanol, 0.2% Triton X-100) and was clarified by centrifugation at 14000 r.p.m. for 15 min. Total protein was measured by the protein-dye binding assay (Bradford, 1976) with the BIO-RAD Protein Assay reagent. Samples (20 μg) were separated on a non denaturing 12.5% polyacrylamide gel at 100 V for 3-4 h. SOD activity was detected on these gels using the *in situ* staining technique of (Beauchamp and Fridovich, 1971). Briefly, the gel was kept in 1 mg/ml NBT for 10 min in the dark and then in developing buffer (33 mM potassium phosphate, pH 7.8, 28 μM riboflavin, 28 mM TEMED) for another 20-min period before exposure to light.

Plasmid constructs

The entire *COPT2* open reading frame was obtained by PCR using the following specific primers: COPT2-SalI-F CATGTCGACATCATGGATCATGATCACATGC AT; COPT2-NcoI-R TCTCCATGGTACAAACGCACCCTGAAGACGGCGGAA. The *COPT2* carboxy terminus was fused in the frame to the *GFP* with the *CaMV35S* promoter through its insertion into transient expression vector P*35SΩsGFP(S65T)* (Miras et al., 2002). *COPT2-GFP*, obtained from the previous construct by PCR using these specific primers: COPT2-HindII-F CATAAGCTTATGGATCATGATCACA TGCAT; GFP-R-SalI CATGTCGACTTACTTGTACAGCTCGTCCAT was cloned into the p426GDP plasmid for the yeast functionality assay. Plasmids p426GDP-*COPT1*

and p426GDP-*COPT2* were described in (Sancenon et al., 2003). The *uidA* coding sequence and the 1248 base pairs from *COPT2* transcription start site (P*COPT2*) (indicated by arrows in Figure S4) were amplified and cloned into the pFP101 plasmid (Bensmihen et al., 2005) without its *CaMV35S* promoter to obtain the P*COPT2:GUS* construct, used to determine the *COPT2* spatial expression pattern by a β-glucuronidase assay. A PCR product containing 1248 bp of the P*COPT2* and the entire *COPT2* coding sequence was cloned into the pFP101 vector and introduced into the *copt2-1* line by floral dipping (Clough and Bent 1998). Homozygous transgenic plants (P*COPT2:COPT2*) were selected based on seed fluorescence. The entire *COPT2* coding sequence was tagged with the human influenza virus haemagglutinin epitope (HA) with the specific primers COPT2-XbaIF CATTCTAGAATGGATCATGATCACATGCAT and COPT2HA-SalI-R ATGTCGACTCAAGCATAATCTGGAACATCGTATGGATAACAAACGCAGCCT GAAGACGGCGGAA and cloned into the pFP101 vector. Transgenic lines were selected based on the fluorescence of the seeds.

Computer-assisted sequence analyses

The hydrophobic profile of the COPT2 protein was obtained by the TMHHM application (www.cbs.dtu.dk/services/TMHHM). The theoretical analysis of the promoter sequences was performed with the PLACE Web Signal Scan (http://www.dna.affrc.go.jp/htdocs/PLACE/signalscan.html) and Patmatch from TAIR (www.arabidopsis.org).

Subcellular localization of the GFP fusion proteins

The Arabidopsis protoplasts from the fresh leaf tissue of the 30-day-old plants grown in soil were transiently transformed with *COPT2-GFP,* as previously described (Abdel-Ghany et al., 2005). After 16 h under continuous light at 23ºC in the wash solution, protoplasts were incubated with the FM4-64 dye (*Invitrogen*) at a concentration of 50 μM for 15 min at 4ºC before analyzing. Confocal images were obtained using a Fluorescence Confocal Microscope TCS SP, vertical (DM-R) (*Leica*), equipped with the Argon ion (458 and 488 nm), He-Ne I (543 nm) and He-Ne II (633 nm) excitation laser systems, and a 40-60X objective lens. Fluorescence signals were detected at 500-530 nm for the GFP, 650-750 nm for chlorophyll and 560-650 nm for FM4-64 after exciting at 488, 633 and 543 nm, respectively.

Immunohistochemical techniques and microscopy

Samples of Arabidopsis plant leaves were fixed in Karnousky reagent. They were dehydrated in successive ethanol series (20%, 40%, 60%, 80%, 95%, and 100%) and embedded in polyethylene glycol for fluorescence microscopy. Semithin sections (2 μM) were placed on slides and rehydratated with xylene and successive ethanol series (100%, 95%, 70%, 0%), washed with PBSII ((PBSI: 137 mM NaCl, 2.7 mM KCl, 9 mM Na_2HPO4, 1.5 mM KH_2PO_4, pH 7.2) + 0.1% BSA and 0.05% Na_2N_3) and dried. Slides were blocked in PBSII with 2% BSA and 1% powder milk for 20 min and dried. Then, labeled overnight at 4ºC and in humidity with rat monoclonal antibody to the HA epitope (clone 3F10; *Roche*) diluted 1:50 in PBSII. Subsequently, washed with PBSI, blocked in PBSII with 2% BSA and 1% powder milk for 20 min and dried. Then, an anti-rat-IgG antibody conjugated with AlexaFluor546 (*Molecular Probes*) diluted 1:500 with 0.1 M Glycine was used for 1-4 h at 4ºC in humidity and darkness. Slides were then washed with PBSI and stained with 1 μg/ml DAPI in PBSI for 5 min. Finally, slides were washed with PBSI and mounted in Citifluor. The fluorescence of immunolabeled COPT2-HA and of DAPI-stained nuclei was visualized with a fluorescence microscope (*Axioskop 2; Zeiss, Jena, Germany*) using the appropriate filter combinations. Micrographs were taken by a camera SPOT (Diagnostic Instruments Inc.) and were processed through the Photoshop program (*Adobe Systems, Seattle*).

Protein analysis by Western blot

A crude extract from the WT and *copt2-1* Arabidopsis leaves grown on plates was obtained and the amount of protein was determined by BCA (the *BCA Protein Assay Kit*, *Thermo*). Next, 40 μg of protein were analyzed by SDS-PAGE, transferred to a nitrocellulose membrane and blotted with an antibody against plastocyanin (*Agrisera*). Coomassie staining was used as a loading control.

GUS expression analyses

Assays were performed as described by (Jefferson et al., 1987). Briefly, the seedlings and organs from the adult P*COPT2:GUS* plants were embedded with the substrate solution [100 mM $NaPO_4$ pH 7.2, 0.5 mM $K_3Fe(CN)_6$, 0.5 mM $K_4Fe(CN)_6$, 0.1% (v/v) Triton X-100, 0.5 mM 5-bromo-4-chloro-3-indolyl-β-D-glucuronide (*X*-

Gluc, AppliChem) and 10 mM EDTA pH 7.2]. Reactions took place at 37ºC and were stopped with ethanol (70%).

copt2-1 mutant line analyses and complementation

The Arabidopsis T-DNA insertion line AL770147 was obtained from the *GABI-Kat Project*. Plants were self-pollinated and an homozygous mutant was obtained (denoted *copt2-1* line). The COPT2-LB (F) and COPT2 RB (R) primers were used to amplify the WT alleles, whereas the COPT2-LB (F) and GKAT-PCR (S) primers amplified the inserted alleles in the *copt2-1* line (see Figure S?A and Table S6). The location of the T-DNA insert was obtained by PCR amplification and sequencing. Several independent lines were obtained from different Arabidopsis databases were checked but none carried a T-DNA insertion in the coding region and the *copt2-1* line was the closest insertion to the *COPT2* coding sequence found among the lines analyzed. A PCR fragment containing the P*COPT2::COPT2* in frame with the *GFP* reporter gene was cloned into the pFP101 plasmid and introduced in the *copt2-1* line by floral dipping to generate a complemented mutant line.

Microarrays and bioinformatics

Four biological replicates (7-day-old seedlings of the WT and *copt2-1* plants grown in the 12L/12D photoperiod) were obtained for each treatment [Fe- and Cu-sufficient medium (+Fe+Cu), Fe-deficient and Cu-sufficient medium (-Fe+Cu) and Fe- and Cu-deficient medium (-Fe-Cu)]. Fe-deficient medium was supplemented with 300 µM ferrozine. Total RNA was isolated using the *RNeasy Plant Mini Kit (Qiagen)* and aRNA was amplified using the *MessageAmp^{TM} II aRNA Amplification kit (Ambion)*. Long oligonucleotide microarrays were provided by Dr. David Galbraith (University of Arizona, http://www.ag.arizona.edu/microarray/). The hybridization and analysis were performed as described elsewhere (Bueso et al., 2007). The expression values ($\log_2$) were obtained using the *GenePix Pro 6.0 microarray-analysis software (Molecular Devices, Sunnyvale CA)* and normalized with the *GenePix Pro 6.0 and Acuity 4.0 software (Molecular Devices, Sunnyvale CA)*. Differential genes were identified with significance analysis of microarray (SAM) (Tusher et al., 2001) with false discovery rate (FDR) of <6% and 2-fold change ($\log_2 \leq |1|$). Biological processes were identified with the Gene Ontology (GO) annotation (Ashburner et al., 2000), performed by the

GeneCodis2.0 (*http://genecodis.dacya.ucm.es/*; (Carmona-Saez et al., 2007; Nogales-Cadenas et al., 2009) programs (Table 1). The total microarray differentially regulated genes are shown as Supplemental material (Tables S1 and S2). The microarray raw data were deposited in the NCBI's Gene Expression Omnibus ibus (Edgar et al., 2002) and are accessible through GEO Series accession number GSE42642**.**

Gene expression by semi-quantitative and real-time quantitative PCR

Total Arabidopsis RNA was extracted with *Trizol Reagent (Ambion)* and RT-PCR was performed with *SSII (Invitrogen),* as previously described (Andres-Colas et al., 2006). RNA was quantified by UV spectrophotometry; its integrity was visually assessed on ethidium bromide-stained agarose gels and was treated with *Dnase I Amp Grade (Invitrogen)*. Semi-quantitative PCR (sqPCR) was carried out with specific oligonucleotides for *ACT1* and *COPT2* (Table S6). Real-time quantitative PCR (qPCR) was carried out with SYBR-Green qPCR Super-Mix-UDG with ROX (*Invitrogen*) and the specific primers detailed in Table S6 were used in a CFX96 Touch^{TM} Real Time PCR Detection System (*BioRad*) with 1 cycle of 95ºC for 2 min and 40 cycles consisting in 95ºC for 30 s and 60ºC for 30 s. Values were normalized to the *UBQ10* mRNA levels and in control conditions WT was used as reference.

Statistical Analysis

The statistical analysis of the relative expression was performed by comparing the relative expression of the genes (RT-PCR) based on the pair wise fixed reallocation randomization test ($P < 0.05$) (Pfaffl et al., 2002); for the remaining parameters, it was carried out using two-way ANOVA with the means compared by the Duncan test ($P \leq 0.05$) using the InfoStat software, version 2010 (http://www.infostat.com.ar; (Di Rienzo et al., 2011).

ACKNOWLEDGEMENTS

We acknowledge the SCSIE (Universitat de València) for the sequencing and confocal microscopy services. We are grateful to Dr. Marinus Pilon for the GFP

plasmid and to Dr. Toshiharu Shikanai for the *spl7* mutant. Finally, we wish to thank Drs Amparo Sanz and Javier Paz-Ares for critically reading the manuscript.

REFERENCES

Abdel-Ghany SE, Muller-Moule P, Niyogi KK, Pilon M, Shikanai T (2005) Two P-type ATPases are required for copper delivery in Arabidopsis thaliana chloroplasts. Plant Cell **17:** 1233-1251

Abel S (2011) Phosphate sensing in root development. Curr Opin Plant Biol **14:** 303-309

Aller SG, Eng ET, De Feo CJ, Unger VM (2004) Eukaryotic CTR copper uptake transporters require two faces of the third transmembrane domain for helix packing, oligomerization, and function. J Biol Chem **279:** 53435-53441

Andres-Colas N, Perea-Garcia A, Puig S, Penarrubia L (2010) Deregulated copper transport affects Arabidopsis development especially in the absence of environmental cycles. Plant Physiol **153:** 170-184

Andres-Colas N, Sancenon V, Rodriguez-Navarro S, Mayo S, Thiele DJ, Ecker JR, Puig S, Penarrubia L (2006) The Arabidopsis heavy metal P-type ATPase HMA5 interacts with metallochaperones and functions in copper detoxification of roots. Plant J **45:** 225-236

Ashburner M, Ball CA, Blake JA, Botstein D, Butler H, Cherry JM, Davis AP, Dolinski K, Dwight SS, Eppig JT, Harris MA, Hill DP, Issel-Tarver L, Kasarskis A, Lewis S, Matese JC, Richardson JE, Ringwald M, Rubin GM, Sherlock G (2000) Gene ontology: tool for the unification of biology. The Gene Ontology Consortium. Nat Genet **25:** 25-29

Beauchamp C, Fridovich I (1971) Superoxide dismutase: improved assays and an assay applicable to acrylamide gels. Anal Biochem **44:** 276-287

Bensmihen S, Giraudat J, Parcy F (2005) Characterization of three homologous basic leucine zipper transcription factors (bZIP) of the ABI5 family during Arabidopsis thaliana embryo maturation. J Exp Bot **56:** 597-603

Bernal M, Casero D, Singh V, Wilson GT, Grande A, Yang H, Dodani SC, Pellegrini M, Huijser P, Connolly EL, Merchant SS, Kramer U (2012) Transcriptome sequencing identifies SPL7-regulated copper acquisition genes FRO4/FRO5 and the copper dependence of iron homeostasis in Arabidopsis. Plant Cell **24:** 738-761

Birkenbihl RP, Jach G, Saedler H, Huijser P (2005) Functional dissection of the plant-specific SBP-domain: overlap of the DNA-binding and nuclear localization domains. J Mol Biol **352:** 585-596

Bradford MM (1976) A rapid and sensitive method for the quantitation of microgram quantities of protein utilizing the principle of protein-dye binding. Anal Biochem **72:** 248-254

Buckhout TJ, Yang TJ, Schmidt W (2009) Early iron-deficiency-induced transcriptional changes in Arabidopsis roots as revealed by microarray analyses. BMC Genomics **10:** 147-163

Bueso E, Alejandro S, Carbonell P, Perez-Amador MA, Fayos J, Belles JM, Rodriguez PL, Serrano R (2007) The lithium tolerance of the Arabidopsis cat2 mutant reveals a cross-talk between oxidative stress and ethylene. Plant J **52:** 1052-1065

Burkhead JL, Reynolds KA, Abdel-Ghany SE, Cohu CM, Pilon M (2009) Copper homeostasis. New Phytol **182:** 799-816

Carmona-Saez P, Chagoyen M, Tirado F, Carazo JM, Pascual-Montano A (2007) GENECODIS: a web-based tool for finding significant concurrent annotations in gene lists. Genome Biol **8:** R3

Castruita M, Casero D, Karpowicz SJ, Kropat J, Vieler A, Hsieh SI, Yan W, Cokus S, Loo JA, Benning C, Pellegrini M, Merchant SS (2011) Systems biology approach in Chlamydomonas reveals connections between copper nutrition and multiple metabolic steps. Plant Cell **23:** 1273-1292

Clough SJ, Bent AF (1998) Floral dip: a simplified method for *Agrobacterium*-mediated transformation of *Arabidopsis thaliana*. Plant J **16:** 735-743

Colangelo EP, Guerinot ML (2004) The essential basic helix-loop-helix protein FIT1 is required for the iron deficiency response. Plant Cell **16:** 3400-3412

Crichton RR, Pierre JL (2001) Old iron, young copper: from Mars to Venus. Biometals **14:** 99-112

Chiou TJ, Lin SI (2011) Signaling network in sensing phosphate availability in plants. Annu Rev Plant Biol **62:** 185-206

Chu CC, Lee WC, Guo WY, Pan SM, Chen LJ, Li HM, Jinn TL (2005) A copper chaperone for superoxide dismutase that confers three types of copper/zinc superoxide dismutase activity in Arabidopsis. Plant Physiol **139:** 425-436

del Pozo T, Cambiazo V, Gonzalez M (2010) Gene expression profiling analysis of copper homeostasis in Arabidopsis thaliana. Biochem Biophys Res Commun **393:** 248-252

Di Rienzo JA, Casanoves F, Balzarini MG, Gonzalez L, Tablada M, Robledo CW (2011) InfoStat.

Duan K, Yi K, Dang L, Huang H, Wu W, Wu P (2008) Characterization of a sub-family of Arabidopsis genes with the SPX domain reveals their diverse functions in plant tolerance to phosphorus starvation. Plant J **54:** 965-975

Edgar R, Domrachev M, Lash AE (2002) Gene Expression Omnibus: NCBI gene expression and hybridization array data repository. Nucleic Acids Res **30:** 207-210

Franco-Zorrilla JM, Valli A, Todesco M, Mateos I, Puga MI, Rubio-Somoza I, Leyva A, Weigel D, Garcia JA, Paz-Ares J (2007) Target mimicry provides a new mechanism for regulation of microRNA activity. Nat Genet **39:** 1033-1037

Garcia-Molina A, Andres-Colas N, Perea-Garcia A, Del Valle-Tascon S, Penarrubia L, Puig S (2011) The intracellular Arabidopsis COPT5 transport protein is required for photosynthetic electron transport under severe copper deficiency. Plant J **65:** 848-860

Guerinot ML (2000) The ZIP family of metal transporters. Biochim Biophys Acta **1465:** 190-198

Hartmann U, Sagasser M, Mehrtens F, Stracke R, Weisshaar B (2005) Differential combinatorial interactions of cis-acting elements recognized by R2R3-MYB, BZIP, and BHLH factors control light-responsive and tissue-specific activation of phenylpropanoid biosynthesis genes. Plant Mol Biol **57:** 155-171

Hermans C, Bourgis F, Faucher M, Strasser RJ, Delrot S, Verbruggen N (2005) Magnesium deficiency in sugar beets alters sugar partitioning and phloem loading in young mature leaves. Planta **220:** 541-549

Hindt MN, Guerinot ML (2012) Getting a sense for signals: regulation of the plant iron deficiency response. Biochim Biophys Acta **1823:** 1521-1530

Hirayama T, Kieber JJ, Hirayama N, Kogan M, Guzman P, Nourizadeh S, Alonso JM, Dailey WP, Dancis A, Ecker JR (1999) RESPONSIVE-TO-ANTAGONIST1, a Menkes/Wilson disease-related copper transporter, is required for ethylene signaling in Arabidopsis. Cell **97:** 383-393

Hirsch J, Marin E, Floriani M, Chiarenza S, Richaud P, Nussaume L, Thibaud MC (2006) Phosphate deficiency promotes modification of iron distribution in Arabidopsis plants. Biochimie **88:** 1767-1771

Ivanov R, Brumbarova T, Bauer P (2012) Fitting into the harsh reality: regulation of iron-deficiency responses in dicotyledonous plants. Mol Plant **5:** 27-42

Jarvis P, Dormann P, Peto CA, Lutes J, Benning C, Chory J (2000) Galactolipid deficiency and abnormal chloroplast development in the Arabidopsis MGD synthase 1 mutant. Proc Natl Acad Sci U S A **97:** 8175-8179

Jefferson RA, Kavanagh TA, Bevan MW (1987) GUS fusions: beta-glucuronidase as a sensitive and versatile gene fusion marker in higher plants. Embo J **6:** 3901-3907

Jeong J, Guerinot ML (2009) Homing in on iron homeostasis in plants. Trends Plant Sci **14:** 280-285

Kampfenkel K, Kushnir S, Babiychuk E, Inze D, Van Montagu M (1995) Molecular characterization of a putative Arabidopsis thaliana copper transporter and its yeast homologue. J Biol Chem **270:** 28479-28486

Kim BE, Nevitt T, Thiele DJ (2008) Mechanisms for copper acquisition, distribution and regulation. Nat Chem Biol **4:** 176-185

Klaumann S, Nickolaus SD, Furst SH, Starck S, Schneider S, Ekkehard Neuhaus H, Trentmann O (2011) The tonoplast copper transporter COPT5 acts as an exporter and is required for interorgan allocation of copper in Arabidopsis thaliana. New Phytol **192:** 393-404

Kobayashi K, Awai K, Nakamura M, Nagatani A, Masuda T, Ohta H (2009) Type-B monogalactosyldiacylglycerol synthases are involved in phosphate starvation-induced lipid remodeling, and are crucial for low-phosphate adaptation. Plant J **57:** 322-331

Liao H, Rubio G, Yan X, Cao A, Brown KM, Lynch JP (2001) Effect of phosphorus availability on basal root shallowness in common bean. Plant Soil **232:** 69-79

Märschner H. (2002) Mineral nutrition in higher plants, Ed Academic Press, London, UK

Miras S, Salvi D, Ferro M, Grunwald D, Garin J, Joyard J, Rolland N (2002) Non-canonical transit peptide for import into the chloroplast. J Biol Chem **277:** 47770-47778

Misson J, Raghothama KG, Jain A, Jouhet J, Block MA, Bligny R, Ortet P, Creff A, Somerville S, Rolland N, Doumas P, Nacry P, Herrerra-Estrella L, Nussaume L, Thibaud MC (2005) A genome-wide transcriptional analysis using Arabidopsis thaliana Affymetrix gene chips determined plant responses to phosphate deprivation. Proc Natl Acad Sci USA **102:** 11934-11939

Murashige TaS, F. (1962) A revised medium for rapid growth and bioassays with tobacco tissue culture. Physiologia plantarum **15:** 473-497

Nevitt T, Ohrvik H, Thiele DJ (2012) Charting the travels of copper in eukaryotes from yeast to mammals. Biochim Biophys Acta **1823:** 1580-1593

Nogales-Cadenas R, Carmona-Saez P, Vazquez M, Vicente C, Yang X, Tirado F, Carazo JM, Pascual-Montano A (2009) GeneCodis: interpreting gene lists through enrichment analysis and integration of diverse biological information. Nucleic Acids Res **37:** W317-322

Palmer CM, Guerinot ML (2009) Facing the challenges of Cu, Fe and Zn homeostasis in plants. Nat Chem Biol **5:** 333-340

Parsons TRaS, J.D. (1962) Oceanic Detritus. Science **136(3513):** 313-314

Pfaffl MW, Horgan GW, Dempfle L (2002) Relative expression software tool (REST) for group-wise comparison and statistical analysis of relative expression results in real-time PCR. Nucleic Acids Res **30:** e36

Penarrubia L, Andres-Colas N, Moreno J, Puig S (2010) Regulation of copper transport in Arabidopsis thaliana: a biochemical oscillator? J Biol Inorg Chem **15:** 29-36

Pilon M, Cohu CM, Ravet K, Abdel-Ghany SE, Gaymard F (2009) Essential transition metal homeostasis in plants. Curr Opin Plant Biol **12:** 347-357

Puig S, Andres-Colas N, Garcia-Molina A, Penarrubia L (2007) Copper and iron homeostasis in Arabidopsis: responses to metal deficiencies, interactions and biotechnological applications. Plant Cell Environ **30:** 271-290

Puig S, Lee J, Lau M, Thiele DJ (2002) Biochemical and genetic analyses of yeast and human high affinity copper transporters suggest a conserved mechanism for copper uptake. J Biol Chem **277:** 26021-26030

Puig S, Penarrubia L (2009) Placing metal micronutrients in context: transport and distribution in plants. Curr Opin Plant Biol **12:** 299-306

Raghothama KG (1999) Phosphate Acquisition. Annu Rev Plant Physiol Plant Mol Biol **50:** 665-693

Rodrigo-Moreno A, Andres-Colas N, Poschenrieder C, Gunse B, Penarrubia L, Shabala S (2012) Calcium- and potassium-permeable plasma membrane transporters are activated by copper in Arabidopsis root tips: linking copper transport with cytosolic hydroxyl radical production. Plant Cell Environ **36:**844-855

Romera FJ, Alcantara E (1994) Iron-Deficiency Stress Responses in Cucumber (Cucumis sativus L.) Roots (A Possible Role for Ethylene?). Plant Physiol **105:** 1133-1138

Sancenon V, Puig S, Mateu-Andres I, Dorcey E, Thiele DJ, Penarrubia L (2004) The Arabidopsis copper transporter COPT1 functions in root elongation and pollen development. J Biol Chem **279:** 15348-15355

Sancenon V, Puig S, Mira H, Thiele DJ, Penarrubia L (2003) Identification of a copper transporter family in Arabidopsis thaliana. Plant Mol Biol **51:** 577-587

Shimojima M, Ohta H (2011) Critical regulation of galactolipid synthesis controls membrane differentiation and remodeling in distinct plant organs and following environmental changes. Prog Lipid Res **50:** 258-266

Stein RJ, Waters BM (2011) Use of natural variation reveals core genes in the transcriptome of iron-deficient Arabidopsis thaliana roots. J Exp Bot **63(2):** 1039-1055

Svistoonoff S, Creff A, Reymond M, Sigoillot-Claude C, Ricaud L, Blanchet A, Nussaume L, Desnos T (2007) Root tip contact with low-phosphate media reprograms plant root architecture. Nat Genet **39:** 792-796

Thibaud MC, Arrighi JF, Bayle V, Chiarenza S, Creff A, Bustos R, Paz-Ares J, Poirier Y, Nussaume L (2010) Dissection of local and systemic transcriptional responses to phosphate starvation in Arabidopsis. Plant J **64:** 775-789

Tusher VG, Tibshirani R, Chu G (2001) Significance analysis of microarrays applied to the ionizing radiation response. Proc Natl Acad Sci U S A **98:** 5116-5121

Ward JT, Lahner B, Yakubova E, Salt DE, Raghothama KG (2008) The effect of iron on the primary root elongation of Arabidopsis during phosphate deficiency. Plant Physiol **147:** 1181-1191

Waters BM, McInturf SA, Stein RJ (2012) Rosette iron deficiency transcript and microRNA profiling reveals links between copper and iron homeostasis in Arabidopsis thaliana. J Exp Bot **63:** 5903-5918

Wintz H, Fox T, Wu YY, Feng V, Chen W, Chang HS, Zhu T, Vulpe C (2003) Expression profiles of Arabidopsis thaliana in mineral deficiencies reveal novel transporters involved in metal homeostasis. J Biol Chem **278:** 47644-47653

Yamasaki H, Abdel-Ghany SE, Cohu CM, Kobayashi Y, Shikanai T, Pilon M (2007) Regulation of copper homeostasis by micro-RNA in Arabidopsis. J Biol Chem **282:** 16369-16378

Yamasaki H, Hayashi M, Fukazawa M, Kobayashi Y, Shikanai T (2009) SQUAMOSA Promoter Binding Protein-Like7 is a central regulator for copper homeostasis in Arabidopsis. Plant Cell **21:** 347-361

Yang TJ, Lin WD, Schmidt W (2010) Transcriptional profiling of the Arabidopsis iron deficiency response reveals conserved transition metal homeostasis networks. Plant Physiol **152:** 2130-2141

Yuan M, Li X, Xiao J, Wang S (2011) Molecular and functional analyses of COPT/Ctr-type copper transporter-like gene family in rice. BMC Plant Biol **11:** 69-81

Table 1. Phosphate-starvation biological process overrepresented in the *copt2-1* line. Common Pi-starvation and *copt2-1* induced genes compared to WT are indicated (Thibaud et al., 2010; *other sources). MIPS codes, gene description, GO cellular function and the microarray values under +Fe+Cu, -Fe-Cu and –Fe+Cu are indicated. The genes used in qRT-PCR quantitation are in bold; the genes statistically significant but with value <1 are in gray; and not statistically significant are indicated as n.s.

MIPS code	Gene description	GO_cellular_function	+Fe+Cu	-Fe-Cu	-Fe+Cu
At2g32960*	PFA-DSP2	catalytic activity, phosphatase activity, protein tyrosine phosphatase activity	2.524	2.873	2.652
At2g04460	unknown	unknown	2.205	2.495	2.300
At5g03545*	**At4**	unknown	1.383	1.986	1.855
At5g20150	**SPX1**	unknown	1.145	1.309	1.477
At1g73010	PPsPase1	phosphoric monoester hydrolase activity	1.073	1.222	1.165
At2g11810	MGD3	1,2-diacylglycerol 3-beta-galactosyltransferase activity	1.306	1.052	0.738
At5g20790	unknown	unknown	0.865	1.811	1.515
At3g09922*	IPS1	unknown	0.614	1.354	1.469
At1g73220	OCT1	carbohydrate and carnitine transporter activity	2.067	0.782	0.733
At3g03530*	NPC4	hydrolase and phospholipase C activity	1.112	0.489	0.607
At1g17710	unknown	phosphoric monoester hydrolase activity	1.448	1.289	n.s.
At1g08310	unknown	galactolipid biosynthetic process, negative regulation of transcription, DNA-dependent	1.000	1.441	n.s.
At4g26530*	unknown	fructose-bisphosphate aldolase activity	1.123	0.219	n.s.
At2g45130	SPX3	unknown	2.069	n.s.	n.s.
At2g30540	unknown	thiol-disulfide exchange intermediate activity	1.039	n.s.	n.s.
At4g11800*	unknown	protein serine/threonine phosphatase activity	n.s.	1.129	n.s.
At1g21980*	PIP5K1	1-phosphatidylinositol-4-phosphate 5-kinase activity	n.s.	n.s.	1.111

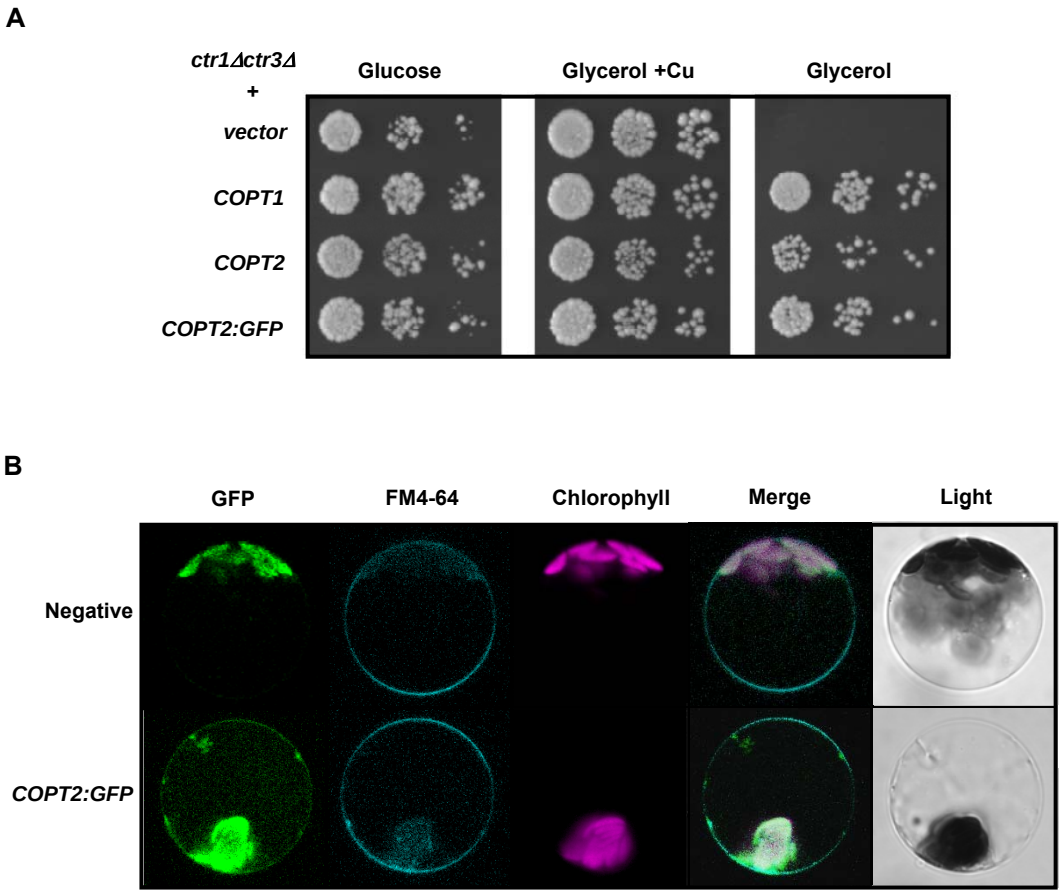

Figure 1. *COPT2:GFP* functionality in yeast and subcellular localization in Arabidopsis protoplasts. A, *Saccharomyces cerevisiae ctr1Δctr3Δ* cells were transformed with p426GPD, *COPT1*, *COPT2* and *COPT2:GFP* and were spotted on SC-ura media (glucose) or YPG (glycerol) supplemented with $CuSO_4$ 100 μM. Each spot represents a 1/10 cell culture density dilution, decreasing from left to right. **B,** Arabidopsis protoplasts were isolated from 30-day-old leaves and were transiently transformed with the P*CaMV35S:COPT2:GFP* construct, incubated with FM4-64 for 15 min at 4ºC before being analyzed by confocal microscopy at 16 h post-transformation. Non transformed protoplasts were used as a negative control. Green, cyan and magenta fluorescences are indicative of the localization of the GFP protein, the FM4-64 marker and chlorophyll, respectively. Representative protoplasts are shown on the same scale, including their merge and light fields.

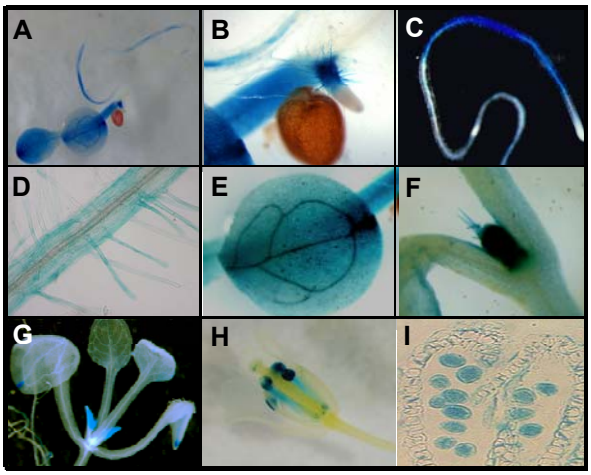

Figure 2. The *COPT2* expression pattern in Arabidopsis P*COPT2:GUS* transgenic plants under Cu deficiency. β-glucuronidase staining in a representative 7-day-old seedling (**A**), detail of a secondary root tip (**B**), general view of the main root (**C**), detail of root hairs (**D**), cotyledon (**E**), shoot meristem and trichomes (**F**), aerial part from a 3-week-old seedling (**G**), flower (**H**) and a longitudinal section of an anther with pollen grains (**I**).

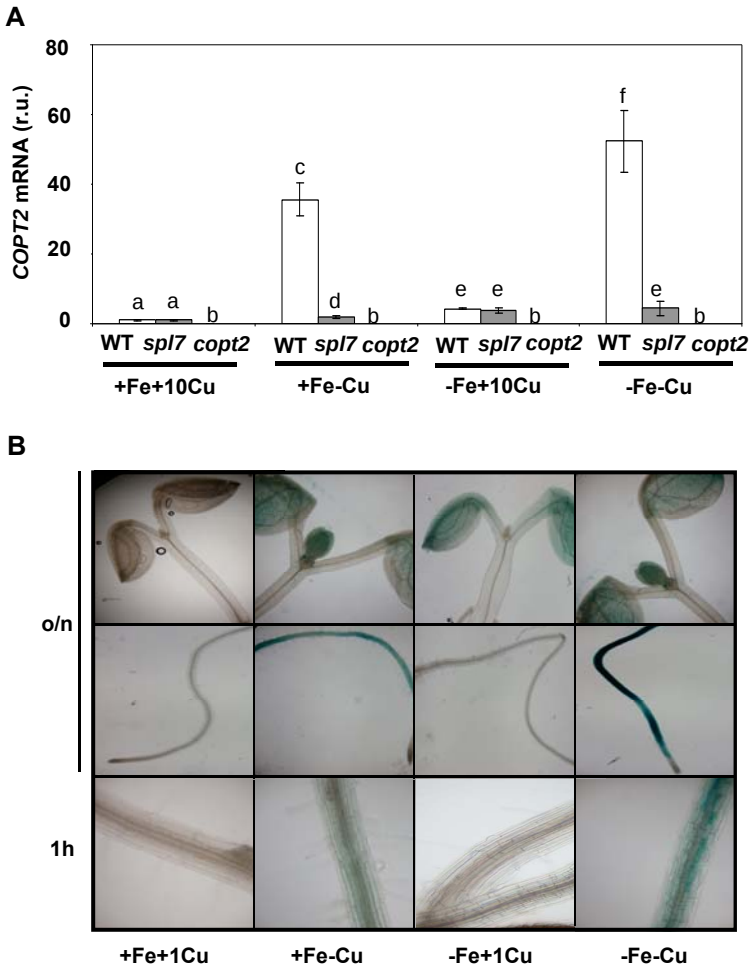

Figure 3. The *COPT2* expression under Cu and Fe deficiencies. **A**, The *COPT2* expression analysis by qPCR in wild-type (WT; plain bars), *spl7* (gray bars) and *copt2-1* (*copt2*; dark gray bars) seedlings. The total RNA from the 7-day-old seedlings grown under the control (+Fe+Cu, supplemented with 10 μM $CuSO_4$), Cu-deficiency (+Fe-Cu), Fe-deficiency (-Fe+Cu, supplemented with 10 μM $CuSO_4$), or Fe and Cu deficiency (-Fe -Cu) conditions described in Materials and Methods was isolated and retrotranscribed to cDNA. The *UBQ10* gene expression was used as a loading control. Values are means ± SD of three biological replicates. r.u., relative units. The different letters above the bars represent significant differences among all the means ($P<0.05$). **B**, β-glucuronidase staining in the 7-day-old seedlings from the P*COPT2:GUS* transgenic lines grown under control (+Fe+Cu, supplemented with 1 μM $CuSO_4$), Cu-deficiency (+Fe-Cu), Fe-deficiency (-Fe+Cu, supplemented with 1 μM $CuSO_4$), or Fe and Cu deficiency (-Fe-Cu) at different incubation times at 37ºC (overnight; o/n and 1hour; 1h).

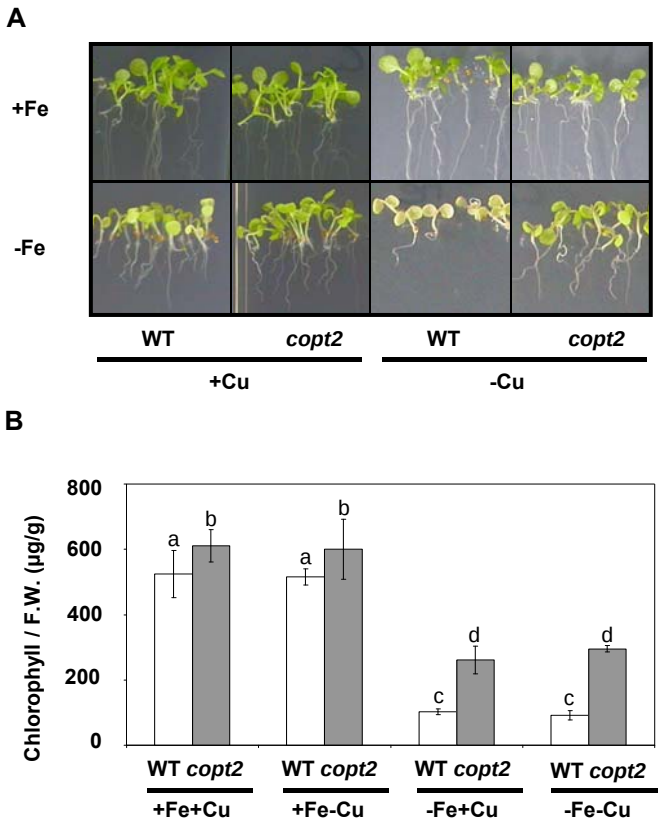

Figure 4. Phenotype of the *copt2-1* seedlings grown under Cu and Fe deficiencies. A, Photographs of the 7-day-old seedlings from the wild type (WT), and *copt2-1* line *(copt2)* grown under the same conditions described in Figure 3A. **B**, Chlorophyll content of the 7-day-old seedlings from both the WT (plain bars) and *copt2* (gray bars) lines grown under the same conditions described in Figure 3. Values are means ± SD of at least three biological replicates. F.W., fresh weight. The different letters above the bars represent significant differences among all the means ($P<0.05$).

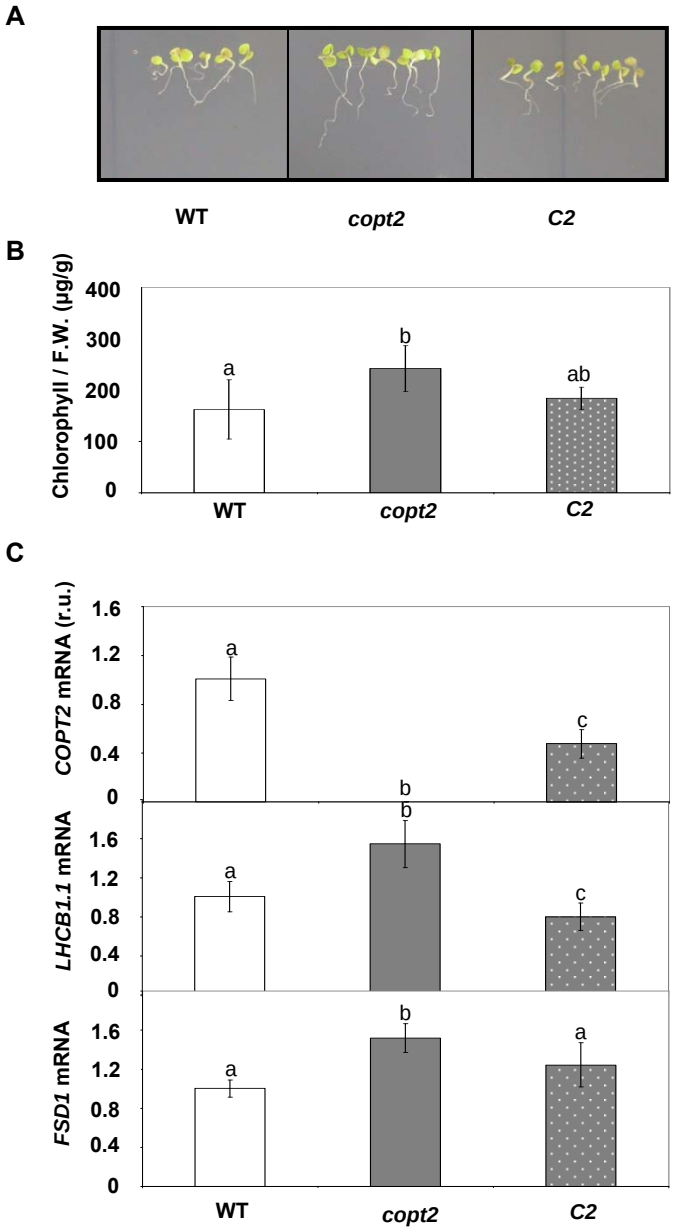

Figure 5. Chlorophyll content and gene expression of complemented *copt2-1* seedlings grown under Cu and Fe deficiencies. A, Photographs of the 7-day-old seedlings from the wild type (WT), *copt2-1* (*copt2*) and P*COPT2:COPT2:GFP* (*C2*) plants grown under -Fe-Cu conditions. **B**, Chlorophyll content of the WT (plain bars), *copt2* (gray bars) and *C2 (*dotted *bars*) seedlings. Values are means ± SD of at least four biological replicates. The different letters above the bars represent significant differences among all the means (P<0.01). **C**, Expression analysis of *COPT2*, *LHCB1.1* and *FSD1* genes by qPCR in WT (plain bars), *copt2* (gray bars) and *C2* (dotted bars) seedlings, as described in Figure 3. The *UBQ10* gene expression was used as a loading control. Values are means ± SD of three biological replicates. r.u., relative units. The different letters above the bars represent significant differences among all the means (P<0.05).

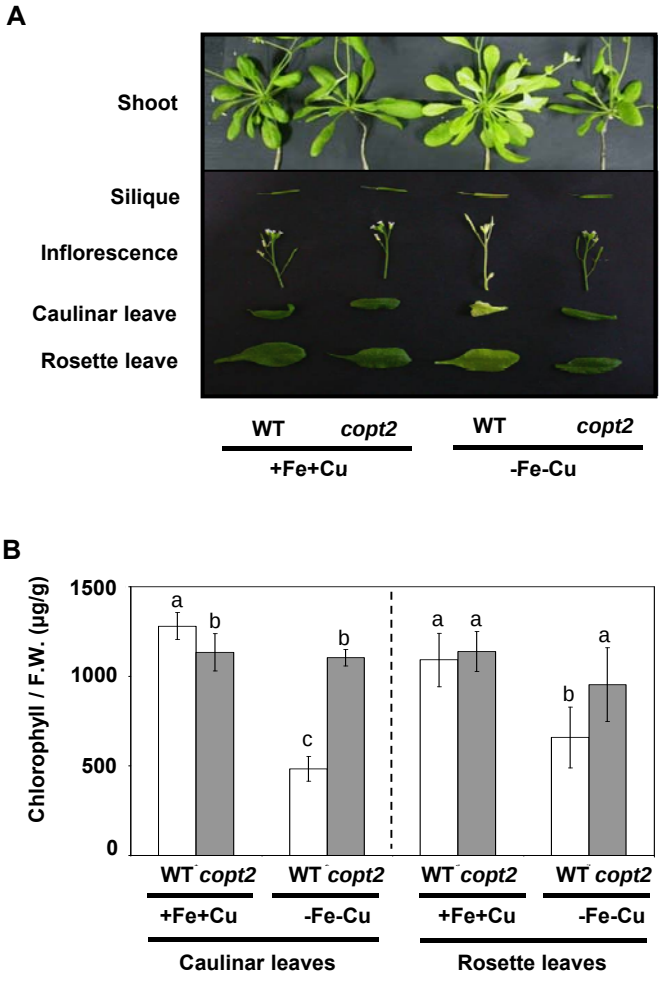

Figure 6. Phenotype of the *copt2-1* adult plants grown under Cu and Fe deficiencies. A, Photographs from the rossette leaves and aerial part details from the wild type (WT) and *copt2-1* line (*copt2*) grown on the +Fe+Cu and -Fe-Cu media were taken 14 days after treatments. **B**, Chlorophyll content of the caulinar and rosette leaves from the WT (plain bars) and *copt2* (gray bars) shown in panel A. Values are means ± SD of four biological replicates. F.W., fresh weight. The different letters above the bars represent significant differences ($P<0.05$) among treatments in a type of leaves.

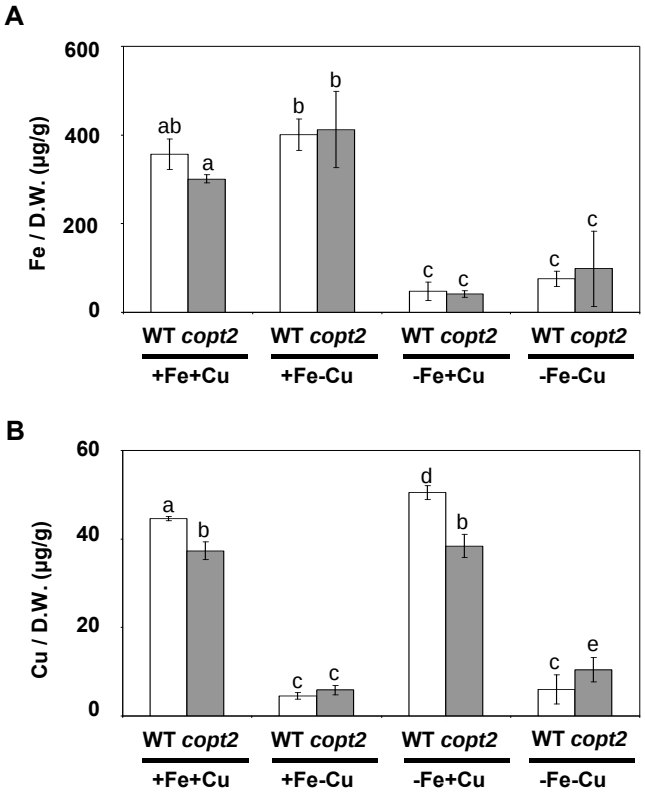

Figure 7. Endogenous Fe and Cu content in WT and *copt2-1* seedlings. Fe (**A**) and Cu (**B**) content were measured by ICP-MS from whole 7-day-old wild type (WT; plain bars) and *copt2-1* (*copt2*; gray bars) plants. Seedlings were grown under the same conditions described in Figure 3. Values are means ± SD of at least three biological replicates. D.W., dried weight. The different letters above the bars represent significant differences among all the means ($P<0.05$).

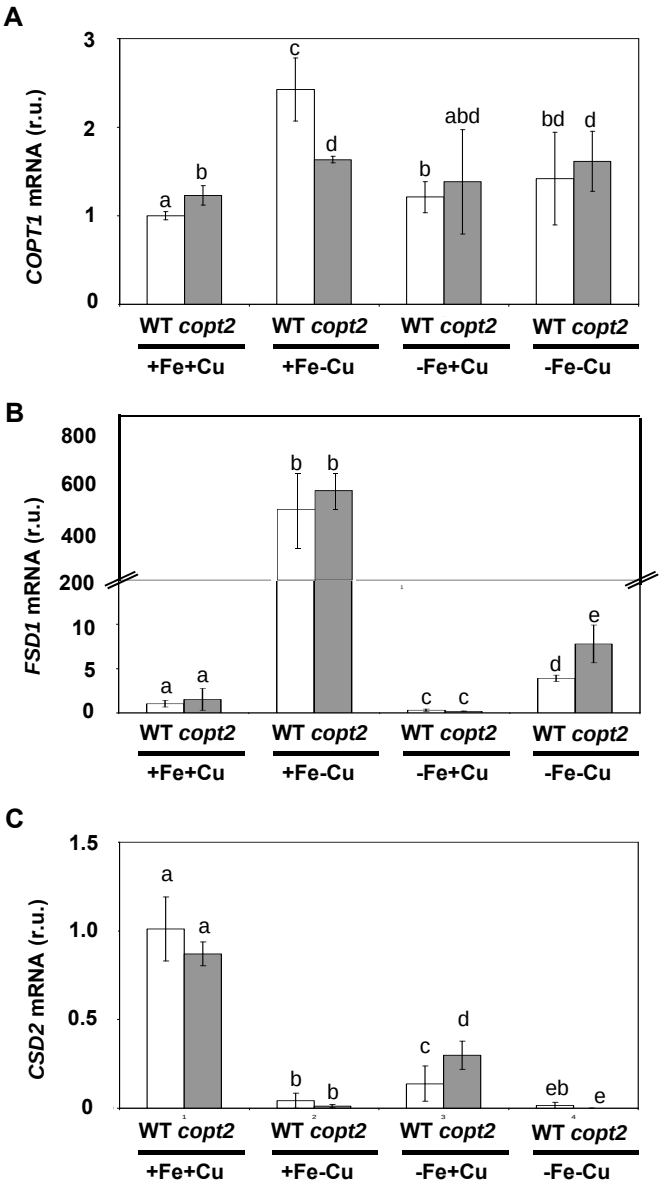

Figure 8. Gene expression pattern of the Cu-deficiency marker genes in the *copt2-1* seedlings. Expression analysis of Cu transporter *COPT1* (**A**), and the Fe and Cu/ZnSOD genes *FSD1* (**B**) and *CSD2* (**C**), respectively, by qPCR in wild type (WT; plain bars) and *copt2-1* (*copt2*; gray bars) seedlings, grown under the same conditions described in Figure 3. The *UBQ10* gene expression was used as a loading control. Values are means ± SD of three biological replicates. r.u., relative units. The different letters above the bars represent significant differences among all the means ($P<0.05$).

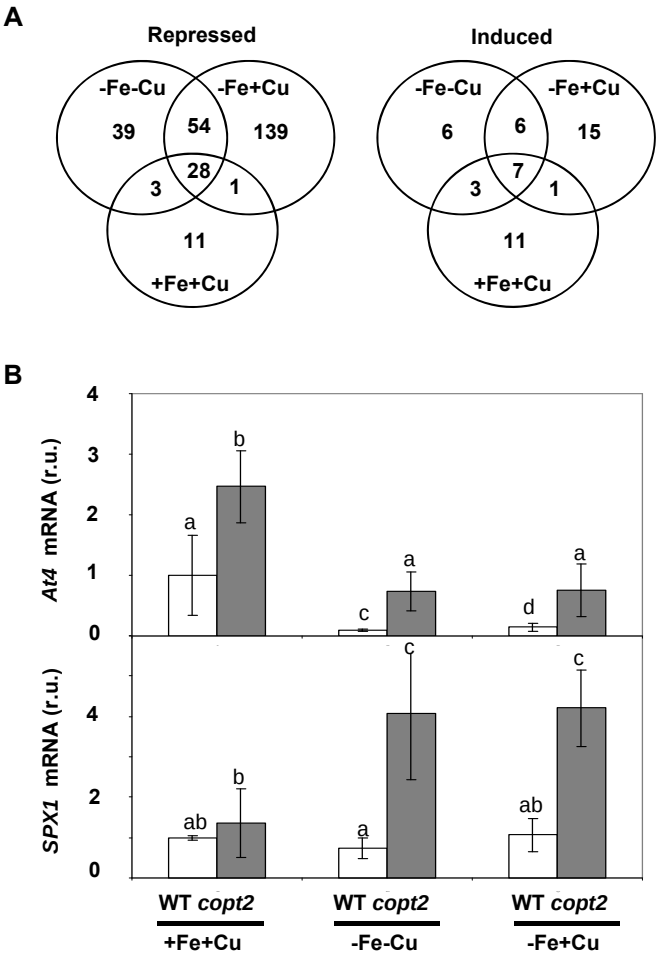

Figure 9. Venn diagrams of gene expression changes in WT versus *copt2-1* seedlings under different metal statuses. A, Numbers indicate the amount of induced/repressed genes under grown under the same conditions described in Figure 3B control (+Fe+Cu), Fe-deficiency (-Fe+Cu) or Fe and Cu deficiency (-Fe -Cu) conditions in *copt2-1* seedlings. **B,** Expression analysis by qPCR of *At4* and *SPX1* in wild type (WT; plain bars) and *copt2-1* (*copt2*; gray bars) seedlings, as described in panel A. The *UBQ10* gene expression was used as a loading control. Values are means ± SD of at least three biological replicates. r.u., relative units. The different letters above the bars represent significant differences among all the means ($P<0.05$).

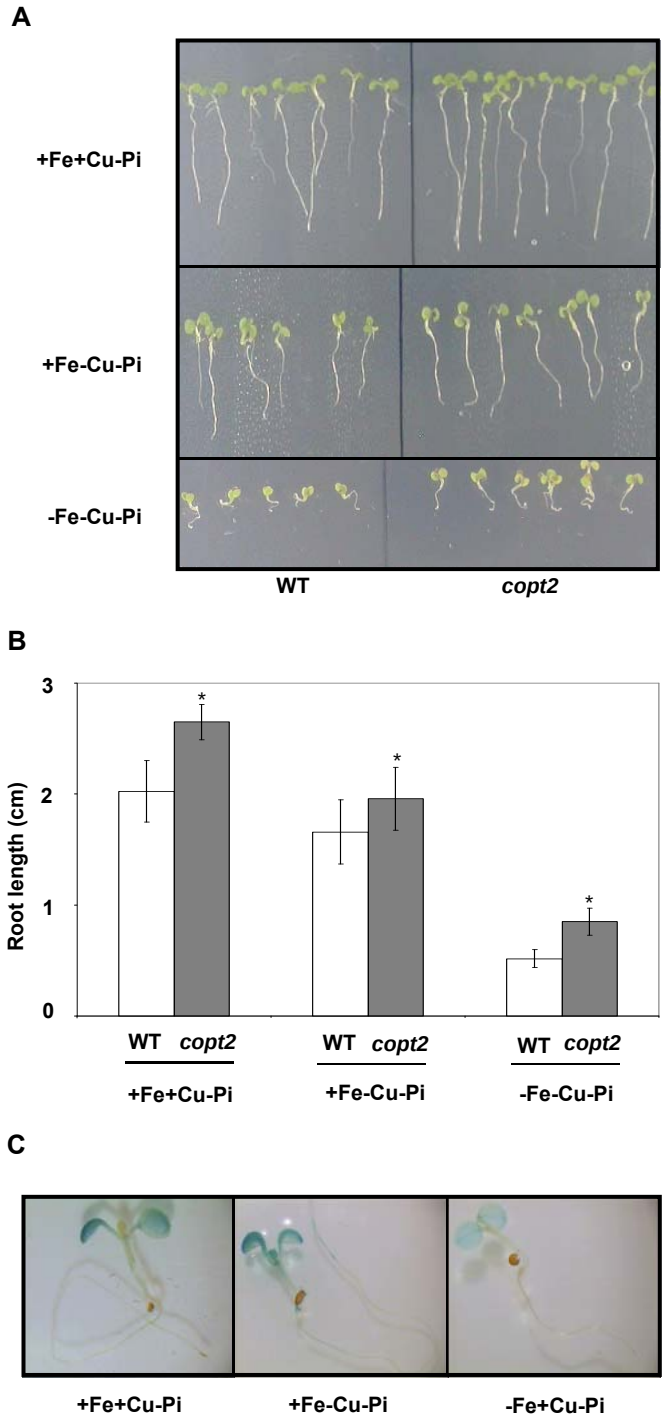

Figure 10. Phenotype of the *copt2-1* seedlings grown under Pi, Cu and Fe deficiencies. A, Representative photographs of the 7-day-old seedlings from the wild type (WT) and *copt2-1* (*copt2*) line grown under Pi starvation (-Pi) and in addition to -Pi, the same conditions described in Figure 3A with regard to Cu deficiency (-Pi-Cu) and Cu and Fe deficiencies (-Pi-Cu-Fe). **B,** Root length from the WT (white bars) and *copt2* (gray bars) measured in three biological replicates ± SD in the samples described in panel A. Asterisks above the bars represent significant differences among all the means ($P<0.05$) comparing to the WT. **C,** Overnight β-glucuronidase staining in the 7-day-old seedlings from the P*COPT2:GUS* transgenic line grown under Pi-deficiency (+Fe+Cu-Pi), Cu and Pi-deficiency (+Fe-Cu-Pi), and Fe and Pi-deficiency (-Fe+Cu-Pi).

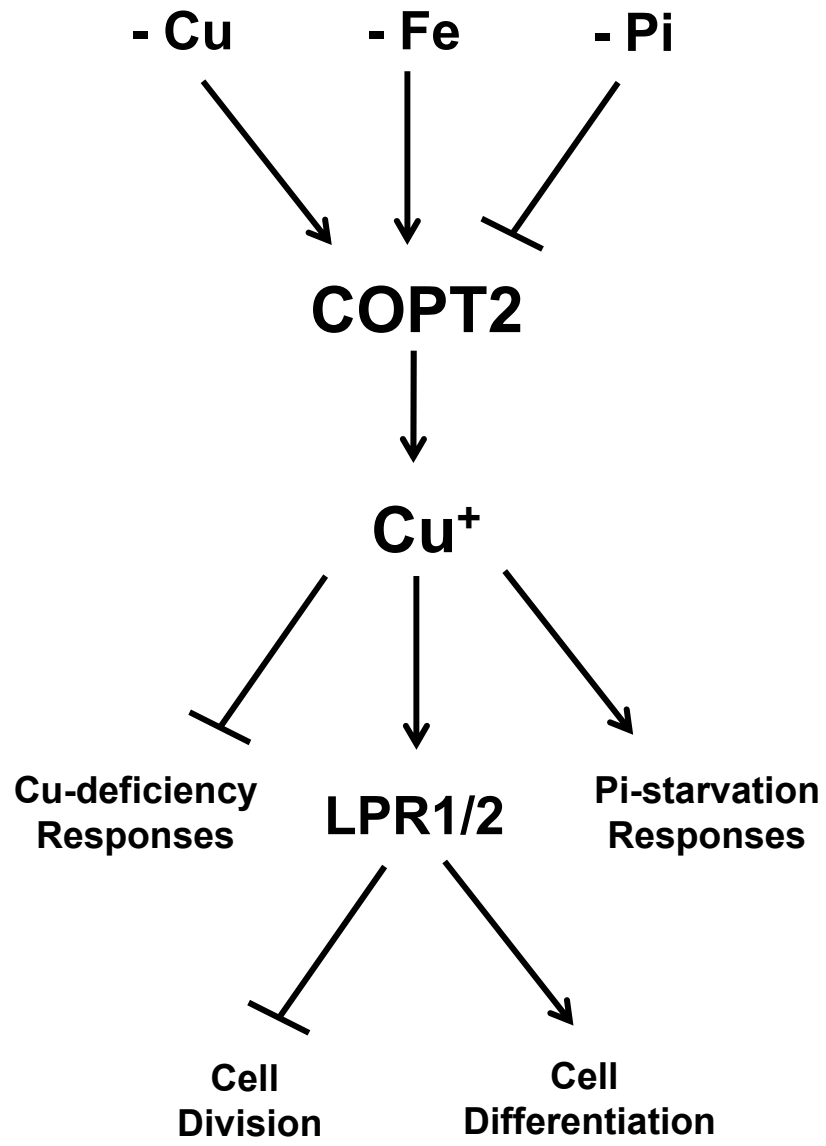

Figure 11. Model of the COPT2-mediated interactions among Cu and Fe deficiencies and Pi starvation responses. Cu, Fe and Pi deficiencies display antagonistic effects on *COPT2* expression. Cu^{+} uptake mediated by COPT2 attenuated Cu deficiency responses, could participate in Cu delivery to low Pi local sensing and systemic signaling. Local sensing mediated by multicopper oxidases LPR1 and LPR2 potentiates cell differentiation versus cell division.